Zeolites

Deutsche Ausgabe: DOI: 10.1002/ange.201504745
Internationale Ausgabe: DOI: 10.1002/anie.201504745

Structure of Nanochannel Entrances in Stopcock-Functionalized Zeolite L Composites

Gloria Tabacchi, Ettore Fois, and Gion Calzaferri**

Abstract: *Multifunctional hybrid materials are obtained by modifying zeolite L (ZL) with stopcock molecules, consisting of a tail group that can enter the ZL nanochannels and a head group too large to pass the channel opening. However, to date no microscopic-level structural information on modified ZL materials has been reported. Herein we draw atomistic pictures of channel openings and stopcock-functionalized ZL based on first-principles calculations. We elucidate the interactions of the tail group with the inner surface of ZL channels and the space-filling properties of the stopcocks, revealing cork- or lid-sealing modes. Water is essential to obtain stable modifications. Al–OH groups are the preferred modification sites, bipodal modifications suffer from strain, and tripod binding is ruled out. Our results suggest the viability of recursive functionalization by cross-linking.*

An impressive variety of composites with a wide range of appealing properties and potential applications, ranging from effect pigments and light harvesting to sensing and diagnostics, has been realized by using the one-dimensional nanochannels of Zeolite L (ZL) as the hosts for ions, complexes, molecules, and nanoparticles.[1–12] In the ZL hexagonal structure, which can be roughly considered as a cylinder, the surface coat and the base have different reactivities. It is therefore possible to selectively modify them to fine-tune the properties of the zeolite.[1,2,4,13–25] Selective modification has been used, for example, for organizing ZL microcrystals into two-dimensional functional entities, such as monolayers, multilayers, and patterned monolayers, on various substrates, thus transferring microscopic qualities to the macroscopic scale.[18,25] Surface hydroxy groups play an important role in these reactions because they allow the attachment of silane coupling agents to the base of ZL.[15,26] These regions bear the channel entrances and are the interface with the outside world: they control the leakage and entrance of guests and determine the composition, stability, and toxicity of the material. Stopcock (or stopper) molecules consisting of a trialkoxysilyl group, too large to pass through the 0.72 nm wide opening of the channel, and a tail group can be attached to ZL with covalent bonds. Some of the alkoxysilane may also adsorb onto the outer cylindrical surface, the amount depending on the reaction conditions. Condensation takes place in solvents containing a quantity of trialkoxysilane sufficient to block the number of channel openings within the dispersed ZL particles. In the first step, the positively charged tail group of the stopcock enters the negatively charged channel by exchanging a charge-compensating cation in an equilibrium reaction. The driving force is trivial ion-exchange free enthalpy resulting from the high concentration of exchangeable K^+ ions in the channel (3.6 per unit cell), while the cations in the solvent are $(R'O)_3SiR^+$. Siloxane bonds with the OH groups of ZL are formed in the next step (usually undertaken in a solvent under reflux). This process endows the modified composite with chemical, photochemical, and thermal stability and is important in the realization of ZL-based multicomponent nanostructures.[4,25–26] It is, however, very difficult to determine experimentally the number of siloxane bonds formed in the condensation reactions, the sites where condensation occurs (Si or Al), and if more than one stopcock can be attached at the same entrance. To answer these questions, we selected two cationic moieties, $AETES^+$ (2-aminoethyltriethoxysilane) and IMZ^+ (*N*-ethyl-*N*′-butylimidazolium trimethoxysilane; Scheme 1), as stopcocks with small and bulky tail groups. Using these molecules we employed first-principles calculations to investigate the interactions of the positively charged tail groups inside the ZL channels, the binding sites, the relative stability of mono-, bi-, and tripod binding, the space-filling properties of the attached stopcocks, and the functionalization of the stopcocks by cross-linking.

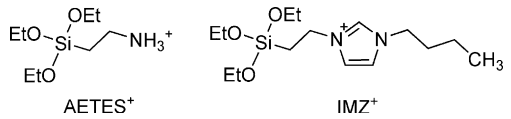

Scheme 1. Structures of $AETES^+$ (2-aminoethyltriethoxysilane) and IMZ^+ (*N*-ethyl-*N*′-butylimidazolium triethoxysilane).

As we aim to understand the interaction of the tail-group moiety with the channel entrance, we chose a computational method suitable for modeling inorganic–organic systems, including dye–ZL composites.[27,28] We optimized the "bottom of the barrel" surface at the channel entrance, which shows 12 Al–OH/Si–OH groups which should be prone to condensation (see the Supporting Information). Stopcock–ZL models were built by adding water (which is always present during ZL modification experiments, sometimes even in large amounts)

[*] Dr. G. Tabacchi, Prof. Dr. E. Fois
Department of Science and High Technology
University of Insubria and INSTM
Via Valleggio 9, 22100 Como (Italy)
E-mail: ettore.fois@uninsubria.it
Prof. Dr. G. Calzaferri
Department of Chemistry and Biochemistry
University of Bern, Freiestrasse 3, 3012 Bern (Switzerland)
E-mail: gion.calzaferri@dcb.unibe.ch

Supporting information for this article is available on the WWW under http://dx.doi.org/10.1002/anie.201504745.

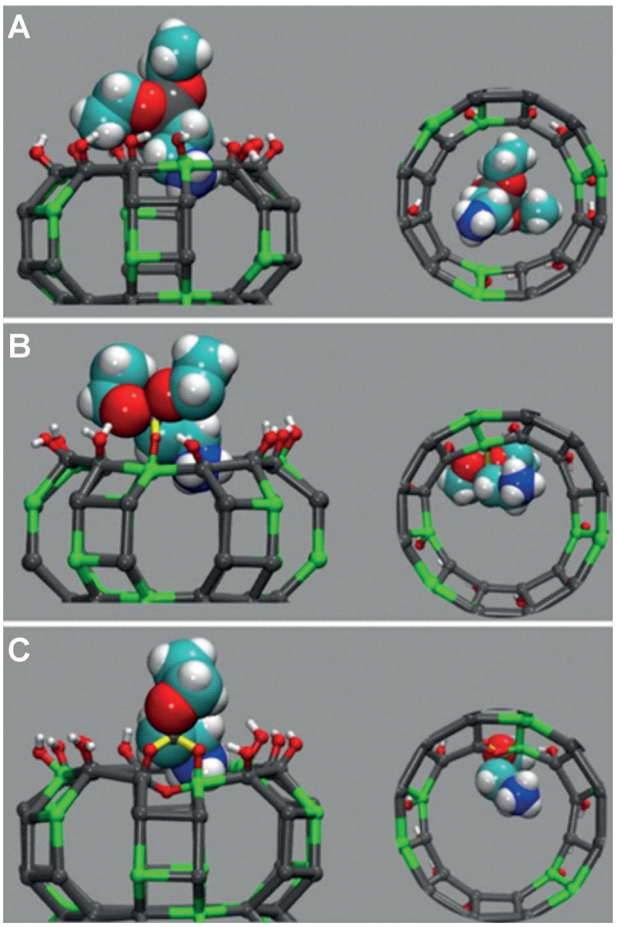

Figure 1. The ZL–AETES$^+$ systems showing the side (left) and bottom (right) views. A) Pre (before bond formation), B) Mpod-Al (monopodal bond formation to Al, one covalent bond), and C) Bipod (bipodal bond formation to Si and Al, two covalent bonds). For clarity, only the T atoms of the ZL framework (T = Si, Al), the ZL hydroxy groups, and the stopcock are shown. Atom colors: Si = gray, Al = green, O = red, H = white, C = cyan, N = blue. The bonds after condensation are shown in yellow.

Table 1: Geometrical parameters and stabilization energies (ΔE).

Model	d(Si–OT) [Å]	α(Si-O-T) [°]	d[a] [Å]	ΔE [b]
AETES$^+$–ZL·2 H_2O:				
Pre	–	–	1.682(S→Z)	−13.5
Mpod-Al	1.634 (Al)	126.9	1.635(S→Z)	−18.1
			1.744(Z→S)	
			1.929(S→Z)	
Mpod-Si	1.657 (Si)	127.0	1.566(S→Z)	−15.0
			1.816(S→Z)	
Bipod	1.643 (Al)	115.0	1.547(S→Z)	−17.1
	1.659 (Si)	119.0	1.799(Z→S)	
			1.987(S→Z)	
IMZ$^+$–ZL·2 H_2O:	1.633 (Al)	128.6	1.746(Z→S)	−1.8
			1.827(Z→S)	
IMZ$^+$–ZL·4 H_2O:	1.633 (Al)	128.1	1.747(Z→S)	−16.1
			1.938(Z→S)	

[a] Hydrogen-bond distances. S→Z denotes hydrogen bonds between stopcock protons and framework oxygen atoms. Z→S denotes hydrogen bonds between ZL hydroxy protons and stopcock oxygen atoms. [b] ΔE values in kcal mol^{-1}.

and replacing a K^+ ion with the stopcock. We begin by discussing the structure of the AETES$^+$–ZL system before condensation (Pre; Figure 1a). In this structure, the siloxane head group of the AETES$^+$ molecule is outside the entrance and partially obstructs the channel. With an ethoxy group close to a ZL hydroxy moiety and the tail group protruding inside, the stopcock is correctly oriented for condensation. Close contact of the tail group with an Al–O–Si bridge of the inner surface (Table 1) suggests that hydrogen bonding and electrostatic interactions orient the stopcock in a geometry suitable for condensation.

To unravel the structure of functionalized ZL, we first attached AETES$^+$ to an Al or a Si site at the channel entrance by a covalent bond, obtaining a stable molecule (ethanol) and a monopodal AETES$^+$–ZL adduct (adducts denoted Mpod-Al and Mpod-Si, respectively). The data in Table 1 shows that condensation leads to a significant stabilization of the structures. Additionally, the greater relative stability of Mpod-Al indicates that the Al–OH moieties are favored modification sites. In this adduct (Figure 1b), the AETES$^+$ tail group forms strong hydrogen bonds with the ZL inner surface and the siloxane head group is hydrogen bonded to the channel opening. Thus, the system is characterized by both strong (covalent) and weak (hydrogen-bonding) interactions. A stabilizing hydrogen-bond network is also formed by water and ZL hydroxy groups at the channel entrance (see the Supporting Information).

To study hydration effects, we added two H_2O molecules to the Mpod-Al system. Energy minimization of the structure positioned the water molecules close to the AETES$^+$ tail group and to a ZL oxygen atom. The ΔE value changed from −18.1 to −23.1 kcal mol^{-1}, indicating that a higher degree of hydration stabilizes the modified ZL materials (see Table S1 in the Supporting Information).

Bipodally attached stopcocks have been postulated to explain the observed blockage of the ZL channels, but no evidence has been put forward.[7,15] We address this question by modeling the bipodal AETES$^+$–ZL system, which shows a ring formed by three T atoms (where T indicates ZL tetrahedral sites, corresponding to Al or Si atoms) joined by three oxygen bridges (3T ring), as shown in Figure 1c. The tail group is hydrogen bonded to a ZL oxygen atom indicating that noncovalent interactions stabilize the bipodal adduct. This adduct also features a strained geometrical arrangement (specifically the 3T ring; the strained structure is probably detectable by employing single-crystal Raman spectroscopy[29]). Larger rings, as well as tripodal binding, are ruled out upon consideration of the O–O separation in AETES$^+$ (2.63 Å): although the distance between neighboring ZL sites is appropriate (2.66 Å), the nearest-neighbor distance (> 5 Å) is too large.

To model complete sealing of the ZL openings, we attached a second AETES$^+$ molecule to Mpod-Al and increased the water content (from two to four molecules) to

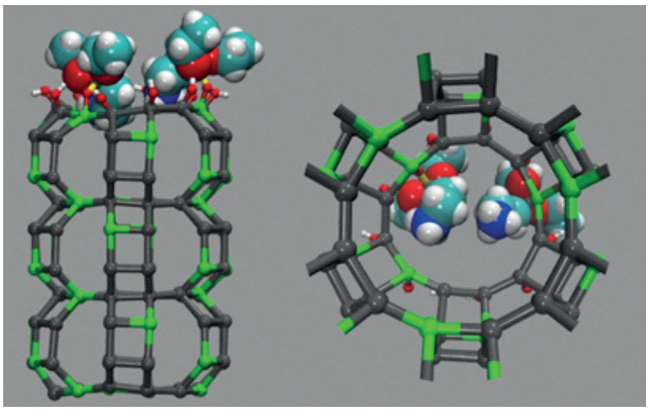

Figure 2. Side (left) and bottom (right) views of ZL functionalized with two $AETES^+$ molecules.

obtain stable bifunctionalized systems. In the most stable structure ($\Delta E = -13.3\ kcal\,mol^{-1}$), both $AETES^+$ molecules are bound at Al sites (Figure 2). Two H_2O molecules lie between the tail groups, whereas the other water molecules participate in the hydrogen-bond network at the channel entrance (see the Supporting Information). A similar arrangement was found by attachment of the second $AETES^+$ molecule to a Si site ($\Delta E = -12.0\ kcal\,mol^{-1}$). These results indicate that modifications of ZL with two $AETES^+$ per channel opening are possible but lead to structures where the positively charged tail groups are in close contact with each other and need further hydration to be stabilized.

As a representative of a stopcock with a bulky tail group we chose the IMZ^+ cation, which has been successfully used in several applications,[2,7] and modeled the IMZ^+–ZL system (Figure 3). Covalent binding of the siloxane head group with ZL hydroxy groups follows the same process as that discussed for $AETES^+$; however, the tail group, now well inside the channel, is not engaged in hydrogen bonds. With two H_2O molecules, the IMZ^+–ZL adduct is less stable than Mpod-Al, whereas with four H_2O molecules the stability of the system was considerably enhanced (Table 1). The new water molecules are hydrogen bonded with the inner surface

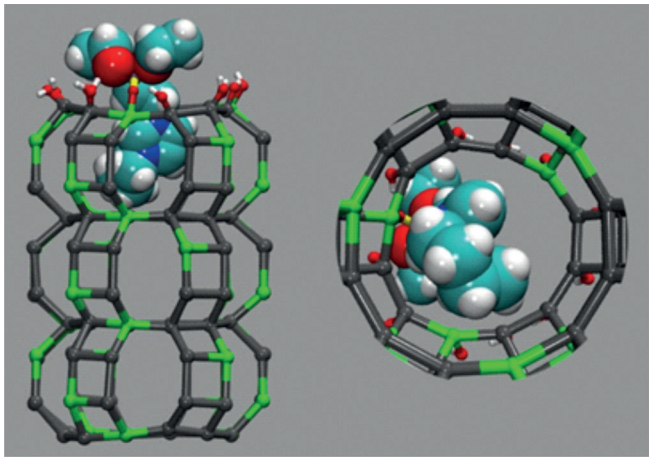

Figure 3. Side (left) and bottom (right) views of the IMZ^+–ZL adduct.

of the channel and are close to the positively charged tail group, thus stabilizing the adduct through hydrogen bonding and electrostatic interactions.

We next discuss the space-filling properties of the models. In contrast to $AETES^+$, the IMZ^+ tail group occupies a larger proportion of the channel entrance and extends far inside the channel (Figure 3). Therefore, it can be considered that IMZ^+ acts like a cork on a bottle: it seals the ZL channel from the inside. Connolly surface representations[30] of the models are particularly informative (Figure 4): upon bonding of IMZ^+,

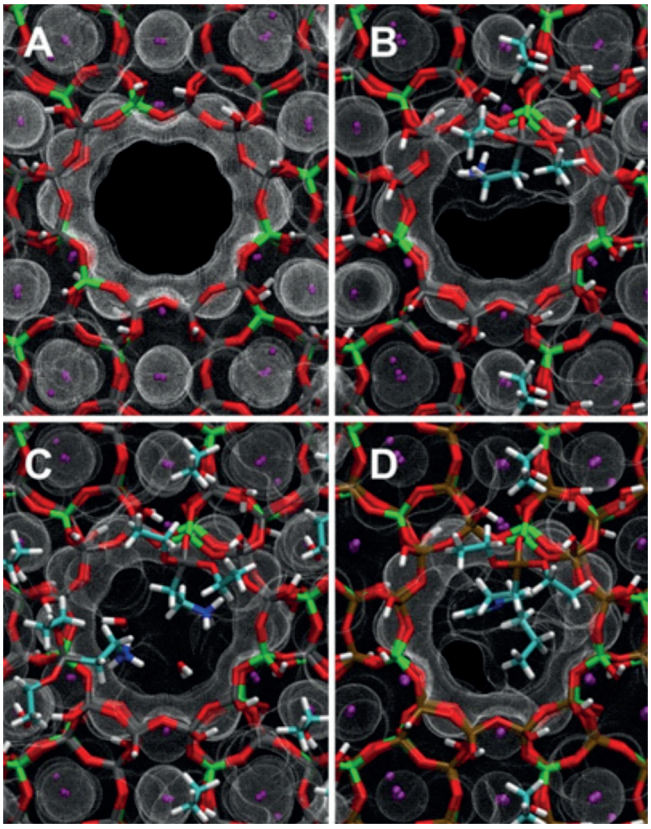

Figure 4. Connolly surfaces (shown as white dots) to of A) unmodified ZL, B) Mpod-Al, C) two $AETES^+$ molecules attached to ZL, and D) IMZ^+–ZL. All atoms are shown as stick models.

the channel entrance is completely blocked. The same effect is observed if two $AETES^+$ molecules are attached. Only small molecules, such as water or ethanol, may enter and no further stopcock can be attached. Nevertheless, the ability of guest molecules to access the channel interior is strongly diminished even with one $AETES^+$ molecule attached. The Connolly surfaces of two dyes used in ZL composites (see the Supporting Information) show that these molecules have cross-sections close in size to the diameter of the channel opening and cannot pass through functionalized ZL channel entrances even if the blockage is only partial, as in Mpod-Al.

In addition to condensation with distinct OH sites, two $AETES^+$ molecules may also undergo cross-condensation processes. We modeled the cross-linking of a neutral AETES

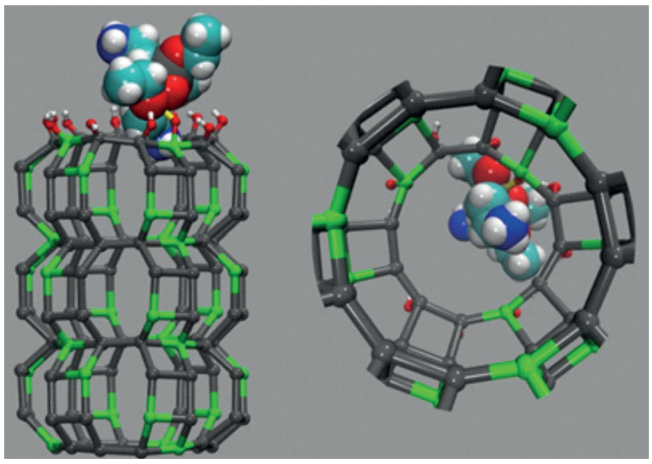

Figure 5. Side (left) and bottom (right) views of the cross-linked ZL model.

to an AETES$^+$-functionalized ZL and obtained a stable adduct (Figure 5). Clearly, modification of the ZL by cross-linking leads to a more effective closure of the channel entrance with respect to Mpod-Al. Whereas the NH_3^+ tail group of the bound stopcock enters the channel, the R-NH_2 group of the linker stays outside. In this geometry, the linker may undergo secondary condensation reactions, for example, with other molecules, nanostructures, or solid supports. Hydrogen bonds within this system are weaker than in Mpod-Al and water plays a key role for stability. Although two H_2O molecules were not sufficient to stabilize the cross-linked model ($\Delta E = +4.4$ kcal mol^{-1}), with four H_2O molecules a stabilization of -20.5 kcal mol^{-1} was calculated.[31]

To address the lack of available microscopic structural information on the site-specific functionalization of ZL, herein we showed how stopper molecules irreversibly modify ZL by condensing with OH groups at the channel entrance. Stoppers with small tail groups behave as partially opened lids and full closure may be achieved by double condensation. On the other hand bulky tail groups seal the entrance like a cork. The importance of stabilization of the systems by hydrogen bonding is highlighted, which explains why water is needed in modification experiments. In this study, new light is shed on the process by which the channels in a nanoporous system may be blocked: a method heavily exploited to create new materials but never captured at the molecular level. By revealing structural information on this process, this work contributes to the fundamental understanding of an important research topic.

Acknowledgements

This work was supported by the Italian MIUR through the projects ImPACT (FIRB RBFR12CLQD), INFOCHEM (PRIN 2010CX2TLM_006), and Insubria FAR2014. The CINECA supercomputing center (Italy) is acknowledged for computing time (ISCRA project DENARI, HP10B6JTDP).

Keywords: density functional calculations · interfaces · nanostructures · supramolecular chemistry · zeolites

How to cite: *Angew. Chem. Int. Ed.* **2015**, *54*, 11112–11116
Angew. Chem. **2015**, *127*, 11264–11268

[1] G. Calzaferri, S. Huber, H. Maas, C. Minkowski, *Angew. Chem. Int. Ed.* **2003**, *42*, 3732–3758; *Angew. Chem.* **2003**, *115*, 3860–3888.
[2] M. Tsotsalas, K. Kopka, G. Luppi, S. Wagner, M. P. Law, M. Schäfers, L. De Cola, *ACS NANO* **2010**, *4*, 342–348.
[3] a) S. Hashimoto, *J. Phys. Chem. Lett.* **2011**, *2*, 509–519; b) G. Schulz-Ekloff, D. Wöhrle, B. van Duffel, R. A. Schoonhey, *Microporous Mesoporous Mater.* **2002**, *51*, 91–138; c) S. Hashimoto, M. Hagiri, N. Matsubara, S. Tobita, *Phys. Chem. Chem. Phys.* **2001**, *3*, 5043–5051.
[4] G. Calzaferri, *Langmuir* **2012**, *28*, 6216–6231.
[5] R. N. Mahato, H. Lülf, M. H. Siekman, S. P. Kersten, P. A. Bobbert, M. P. de Jong, L. De Cola, W. G. van der Wiel, *Science* **2013**, *341*, 257–260.
[6] a) T. Wen, W. Zhang, X. Hu, L. He, H. Li, *ChemPlusChem* **2013**, *78*, 438–442; b) A. Mech, A. Monguzzi, F. Meinardi, J. Mezyk, G. Macchi, R. Tubino, *J. Am. Chem. Soc.* **2010**, *132*, 4574–4576.
[7] a) P. Li, Y. Wang, H. Li, G. Calzaferri, *Angew. Chem. Int. Ed.* **2014**, *53*, 2904–2909; *Angew. Chem.* **2014**, *126*, 2948–2953; b) P. Cao, O. Khorev, A. Devaux, L. Sägesser, A. Kunzmann, A. Ecker, D. Brühwiler, R. Häner, G. Calzaferri, P. Belser, unpublished results.
[8] Z. Li, J. Hüve, C. Krampe, G. Luppi, M. Tsotsalas, J. Klingauf, L. De Cola, K. Riehemann, *Small* **2013**, *9*, 1809–1820.
[9] H. Manzano, L. Gartzia-Rivero, J. Bañuelos, I. López-Arbeloa, *J. Phys. Chem. C* **2013**, *117*, 13331–13336.
[10] R. Bartolomeu, R. Bértolo, S. Casale, A. Fernandes, C. Henriques, P. da Costa, F. Ribeiro, *Microporous Mesoporous Mater.* **2013**, *169*, 137–147.
[11] A. Devaux, G. Calzaferri, I. Miletto, P. Cao, P. Belser, D. Brühwiler, O. Khorev, R. Häner, A. Kunzmann, *J. Phys. Chem. C* **2013**, *117*, 23034–23047.
[12] A. Devaux, G. Calzaferri, P. Belser, P. Cao, D. Brühwiler, A. Kunzmann, *Chem. Mater.* **2014**, *26*, 6878–6885.
[13] H. Maas, G. Calzaferri, *Angew. Chem. Int. Ed.* **2002**, *41*, 2284–2288; *Angew. Chem.* **2002**, *114*, 2389–2392.
[14] O. Bossart, L. De Cola, S. Welter, G. Calzaferri, *Chem. Eur. J.* **2004**, *10*, 5771–5775.
[15] T. Ban, D. Brühwiler, G. Calzaferri, *J. Phys. Chem. B* **2004**, *108*, 16348–16352.
[16] N. Vilaça, R. Amorim, A. F. Machado, P. Parpot, M. F. R. Pereira, M. Sardo, J. Rocha, A. M. Fonseca, I. C. Neves, F. Baltazar, *Colloids Surf. B* **2013**, *112*, 237–244.
[17] B. Schulte, M. Tsotsalas, M. Becker, A. Studer, L. De Cola, *Angew. Chem. Int. Ed.* **2010**, *49*, 6881–6884; *Angew. Chem.* **2010**, *122*, 7033–7036.
[18] S. Hashimoto, K. Samata, T. Shoji, N. Taira, T. Tomita, S. Matsuo, *Microporous Mesoporous Mater.* **2009**, *117*, 220–227.
[19] C. Sprung, B. M. Weckhuysen, *J. Am. Chem. Soc.* **2015**, *137*, 1916–1928.
[20] I. López-Duarte, L.-Q. Dieu, I. Dolamic, M. V. Martínez-Díaz, T. Torres, G. Calzaferri, D. Brühwiler, *Chem. Eur. J.* **2011**, *17*, 1855–1862.
[21] A. Szarpak-Jankowska, C. Burgess, L. De Cola, J. Huskens, *Chem. Eur. J.* **2013**, *19*, 14925–14930.
[22] a) M. Grüner, M. V. Siozios, B. Hagenhoff, D. Breitenstein, C. A. Strassert, *Photochem. Photobiol.* **2013**, *89*, 1406–1412; b) A. Bertucci, H. Lülf, D. Septiadi, A. Manicardi, R. Corradini, L. De Cola, *Adv. Healthcare Mater.* **2014**, *3*, 1812–1817.
[23] a) J. M. Beierle, R. Roswanda, P. M. Erne, A. C. Coleman, W. R. Browne, B. L. Feringa, *Part. Part. Syst. Charact.* **2013**, *30*, 273–

279; b) S. Huber, G. Calzaferri, *Angew. Chem. Int. Ed.* **2004**, *43*, 6738 – 6742; *Angew. Chem.* **2004**, *116*, 6906 – 6910.
[24] F. Cucinotta, A. Guenet, C. Bizzarri, W. Mróz, C. Botta, B. Milián-Medina, J. Gierschner, L. De Cola, *ChemPlusChem* **2014**, *79*, 45 – 57.
[25] a) A. Zabala Ruiz, H. Li, G. Calzaferri, *Angew. Chem. Int. Ed.* **2006**, *45*, 5282 – 5287; *Angew. Chem.* **2006**, *118*, 5408 – 5413; b) F. Cucinotta, Z. Popovic, E. A. Weiss, G. M. Whitesides, L. De Cola, *Adv. Mater.* **2009**, *21*, 1142 – 1145; c) P. Cao, Y. Wang, H. Li, X. Yu, *J. Mater. Chem.* **2011**, *21*, 2709 – 2714; d) K. B. Yoon, *Acc. Chem. Res.* **2007**, *40*, 29 – 40; e) V. Vohra, A. Bolognesi, G. Calzaferri, C. Botta, *Langmuir* **2009**, *25*, 12019 – 12023; f) Y. Wang, H. Li, Y. Feng, H. Zhang, G. Calzaferri, T. Ren, *Angew. Chem. Int. Ed.* **2010**, *49*, 1434 – 1438; *Angew. Chem.* **2010**, *122*, 1476 – 1480; g) N. S. Kehr, B. Ergün, H. Lülf, L. De Cola, *Adv. Mater.* **2014**, *26*, 3248 – 3252.
[26] a) J. S. Park, Y.-J. Lee, K. B. Yoon, *J. Am. Chem. Soc.* **2004**, *126*, 1934 – 1935; b) A. Kulak, Y.-J. Lee, Y. S. Park, K. B. Yoon, *Angew. Chem. Int. Ed.* **2000**, *39*, 950 – 953; *Angew. Chem.* **2000**, *112*, 980 – 983.
[27] a) E. Fois, G. Tabacchi, G. Calzaferri, *J. Phys. Chem. C* **2010**, *114*, 10572 – 10579; b) E. Fois, G. Tabacchi, G. Calzaferri, *J. Phys. Chem. C* **2012**, *116*, 16784 – 16799; c) E. Fois, G. Tabacchi, A. Devaux, P. Belser, D. Brühwiler, G. Calzaferri, *Langmuir* **2013**, *29*, 9188 – 9198; d) X. Zhou, T. A. Wesolowski, G. Tabacchi, E. Fois, G. Calzaferri, A. Devaux, *Phys. Chem. Chem. Phys.* **2013**, *15*, 159 – 167.
[28] a) L. Gigli, R. Arletti, G. Tabacchi, E. Fois, J. G. Vitillo, G. Martra, G. Agostini, S. Quartieri, G. Vezzalini, *J. Phys. Chem. C* **2014**, *118*, 15732 – 15743; b) A. Gamba, G. Tabacchi, E. Fois, *J. Phys. Chem. A* **2009**, *113*, 15006 – 15015; c) E. Fois, G. Tabacchi, D. Barreca, A. Gasparotto, E. Tondello, *Angew. Chem. Int. Ed.* **2010**, *49*, 1944 – 1948; *Angew. Chem.* **2010**, *122*, 1988 – 1992; d) G. Tabacchi, E. Fois, D. Barreca, A. Gasparotto, *Int. J. Quantum Chem.* **2014**, *114*, 1 – 7; e) G. Tabacchi, E. Fois, D. Barreca, A. Gasparotto, *Phys. Status Solidi A* **2014**, *211*, 251 – 259.
[29] P. Bornhauser, G. Calzaferri, *J. Phys. Chem.* **1996**, *100*, 2035 – 2044.
[30] M. L. Connolly, *J. Appl. Crystallogr.* **1983**, *16*, 548 – 558.
[31] All calculations were performed with the code CPMD: Car – Parrinello Molecular Dynamics, Version 3.17.1, IBM Corp. **1990 – 2015** and MPI für Festkörperforschung Stuttgart **1997 – 2001** (www.cpmd.org).

Received: May 26, 2015
Published online: August 7, 2015